Int. J. Electrochem. Sci., 11 **(2016)** 2345 - 2359

International Journal of
ELECTROCHEMICAL
SCIENCE
www.electrochemsci.org

Effect of Inorganic Anions on the Pitting Behaviour of Austenitic Stainless Steel 304 in H_2SO_4 Solution Containing Chloride Ion

M. Saadawy

Chemistry department, faculty of science, alexandria university, ibrahimia, p.o. box 426, Alexandria, 21321, egypt
E-mail: marwan.saadawy@yahoo.com

Received: 24 July 2015 / *Accepted:* 11 November 2015 / *Published:* 1 February 2016

The effect of addition of inorganic anions, silicate, periodate and permanganate on the pitting behavior of stainless steel 304 in 0.5M H_2SO_4 containing 0.1M NaCl was studied using electrochemical impedance spectroscopy (EIS) and potentiodynamic polarization techniques. In the absence and presence of silicate ion, the peak characteristic for the reduction of sulphate ion was clear in the potentiodynamic polarization curve. This peak was also present in presence of low concentrations of periodate or permanganate but disappeared at high concentrations of both anions. This indicates that periodate or permanganate ions possess a great pitting inhibition at high concentrations, this was also confirmed by EIS technique.

Keywords: A. stainless steel; B. polarization; B. EIS; C. pitting corrosion.

1. INTRODUCTION

Stainless steels are important class of metals and are often considered as the main part of modern industry [1] such as oil and petrochemical industry and also for designing different parts in desalination plants and have been employed as a substitutional metal for carbon steel in highly corrosive media [2], this is attributed to their high corrosion resistance resulting from the high chromium content that contributes to form a highly stable and adherent oxide film which prevents rust formation. At least 12 wt% of chromium is necessary to make steel eligible to be classified as "stainless steel" [3]. Austenitic stainless steel (300 series) is considered as the most important group [4] among all groups of stainless steel since they are characterized by their excellent mechanical properties. Austenitic stainless steel is characterized by high corrosion resistance in various corrosion

conditions without the addition of any other protective agents. It is characterized by excellent work-hardening and mechanical ductility, which makes it suitable for many industrial processes [4,5] and is not fragile in traditional applications [6]. Austenitic stainless steels are the most important alloys utilized in industrial applications that require corrosion resistant materials which are susceptible to stress corrosion cracking in environments that contain corrosive ions in presence of tensile stress. Pitting corrosion in different situations is considered as an important technological problem since it causes the failure of stainless steels. Nowadays, there is a new trend to exploit several types of inhibitors for the corrosion of stainless steels [7]. Acid solutions that contain chloride ions may destroy their passivity with subsequent pitting formation so a great effort is now concentrated to resolve the problem of localized corrosion of stainless steels in chloride-containing media [8–16] and its inhibition [17-19]. The effect of inorganic anions on the pitting of different stainless steels was investigated [20-26] using potentiostatic and potentiodynamic polarization techniques. The aim of the present work is to study the effect of addition of different inorganic anions on the corrosion of stainless steel 304 in 0.5M H_2SO_4 containing 0.1M NaCl using electrochemical impedance spectroscopy (EIS) and potentiodynamic polarization techniques.

2. EXPERIMENTAL

Potentiodynamic polarization and EIS measurements were performed using frequency response analyzer Gill AC instrument. Polarization measurements were carried out at scan rate of 30mV/min. The electrochemical measurements were done in a three-electrode-mode cell; saturated calomel electrode (SCE) and platinum sheet electrode were utilized as reference and counter electrodes respectively. The working electrode was stainless steel 304 (or 304 SS) that had the chemical composition (wt %): 18.25 Cr, 8.5 Ni, 0.58 Mn, 1.17 Mo, 0.06 Ti, 0.02 Al, 0.06 V, 0.005 S, 0.17 C, 0.11 Cu and balance Fe.

The stainless steel samples were fixed in poly tetrafluoro ethylene (PTFE) rods using an epoxy resin so that only one surface remained uncovered. The exposed area (1 cm^2) was mechanically polished with a series of emery papers starting with a coarse one till reaching the finest (800) grade. The samples were then washed thoroughly with double distilled water followed by A.R. ethanol and finally with distilled water and then inserted in the cell.

2.1. Solution Preparation

H_2SO_4, Solids NaCl, $Na_2SiO_3.5H_2O$, $NaIO_4$, $KMnO_4$ are purchased from Aldrich Chemicals Company. Solutions were prepared utilizing double distilled water. Stock solutions of 2M H_2SO_4, 1M NaCl, 0.1M $Na_2SiO_3.5H_2O$, 0.1M $NaIO_4$, 0.1M $KMnO_4$ solutions were used to prepare solutions containing 0.5M H_2SO_4, 0.1M NaCl and the desired concentration of anions using appropriate dilutions. Stock solution concentration was expressed in term of moles/dm^3.

3. RESULTS AND DISCUSSION

3.1. Potentiodynamic Polarization Results

Figure 1 shows the potentiodynamic polarization curves of 304 SS in 0.5M H_2SO_4 containing 0.1M NaCl. The Figure shows bistable behavior [27] in which the metal undergoes anodic dissolution followed by passivation then by anodic passive dissolution which intersects with the cathodic sulphate reduction giving rise to secondary open circuit potential (OCP) similar to that appears in the dissolution of 304 SS exposed to nitric acid in presence of sodium chloride [28] due to the mixed potential of anodic passive dissolution and cathodic NO_3^- and/or NO_2 reduction. In a previous work [29], similar shape of potentiodynamic polarization curve was obtained for 304 SS in 0.5M H_2SO_4 containing different sodium chloride concentrations and the variation of pitting potential of the metal was studied as a function of sodium chloride concentration.

Figure 2 reveals the potentiodynamic polarization curves of 304 SS in 0.5M H_2SO_4 containing 0.1M NaCl in the absence and presence of high concentration, 10^{-2} M of $Na_2SiO_3.5H_2O$, it is clear that in the absence or presence of silicate ion, the polarization curve is characterized by the presence of the secondary OCP which is due to the mixed potential of anodic dissolution of metal and cathodic sulphate reduction indicating that the addition of high concentration of silicate ion has not diminished the reduction of sulphate hence a small or moderate efficiency of inhibition is predicted for the pitting process of metal in presence of silicate.

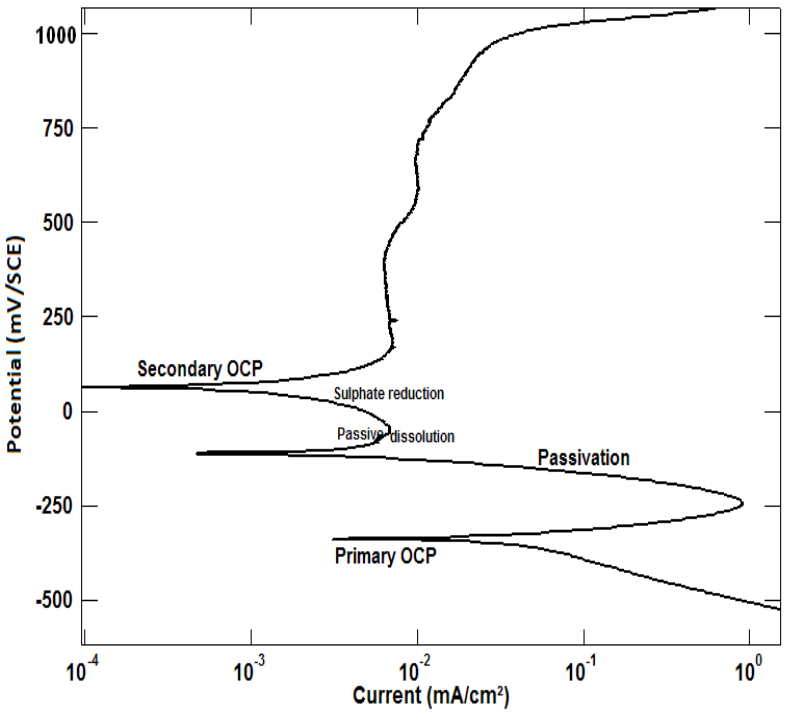

Figure 1. Potentiodynamic polarization curves of 304 SS in 0.5M H_2SO_4 containing 0.1M NaCl.

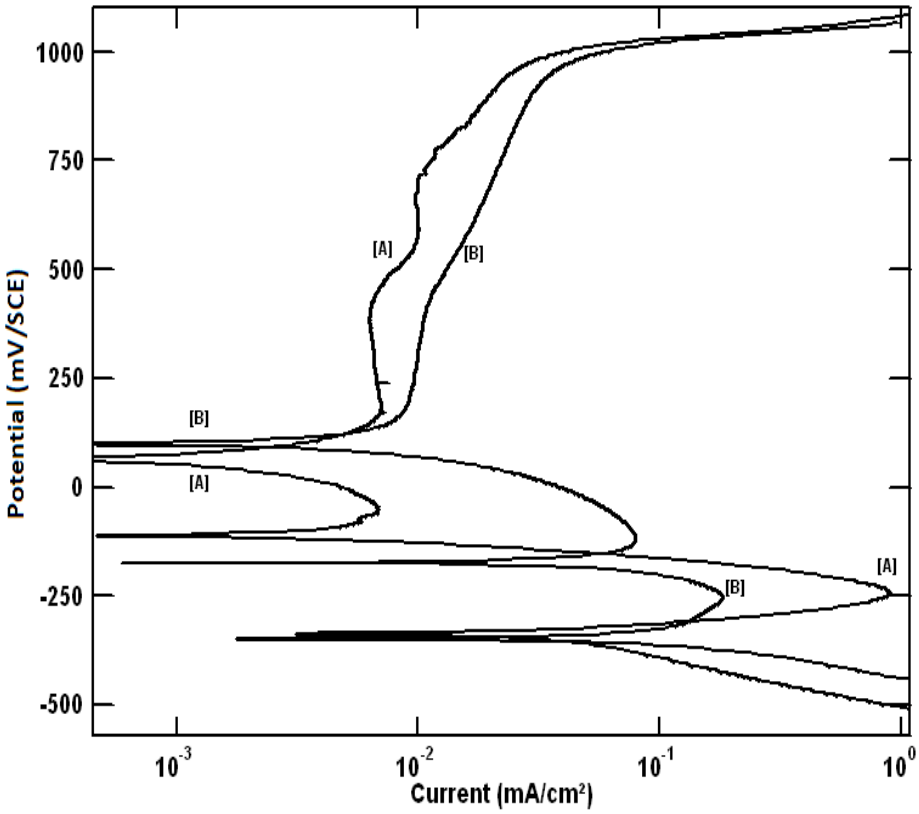

Figure 2. Potentiodynamic polarization curves of 304 SS in [A] 0.5M H_2SO_4 + 0.1M NaCl, [B] 0.5M H_2SO_4 + 0.1M NaCl +10^{-2}M $Na_2SiO_3.5H_2O$.

Figures 3,4 show the potentiodynamic polarization curves of 304 SS in 0.5M H_2SO_4 containing 0.1M NaCl in the absence and presence of 10^{-4}M $NaIO_4$ and $KMnO_4$ respectively. The polarization curves are characterized by the presence of secondary OCP indicating that the presence of low concentration of periodate or permanganate does not diminish the sulphate reduction.

Figures 5,6 show the potentiodynamic polarization curves of 304 SS in 0.5M H_2SO_4 containing 0.1M NaCl in the absence and presence of different higher concentrations of $NaIO_4$ or $KMnO_4$ respectively. it is shown that the presence of high concentration of periodate or permanganate causes the disappearance of the secondary OCP indicating that the high concentration of both anions inhibit the 304 SS corrosion by preventing the cathodic reduction of sulphate accompanying the pitting process and hence achieving high inhibition efficiency for the pitting of metal. The pitting corrosion of stainless steel 304 was found [30] to be reduced in acidified chloride solutions by chromate or molybdate ions by affecting the nucleation of pitting process and metastable pitting by reducing the numbers and sizes of these events while in acid solutions, the pitting inhibition of 304 SS by ions was attributed [31] to promoting enhanced passivation or by organic inhibitors due to the formation of very low soluble layer on the metal surface [32].

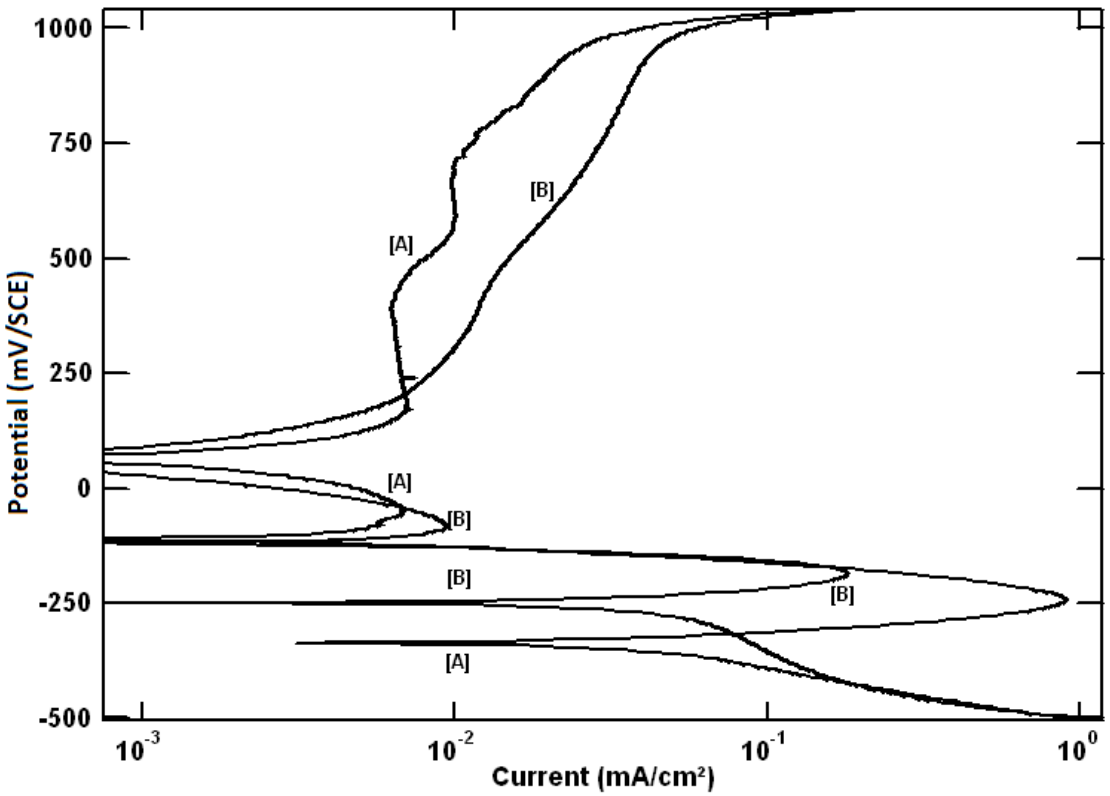

Figure 3. Potentiodynamic polarization curves of 304 SS in [A] 0.5M H_2SO_4 + 0.1M NaCl, [B] 0.5M H_2SO_4 + 0.1M NaCl + 10^{-4}M of $NaIO_4$.

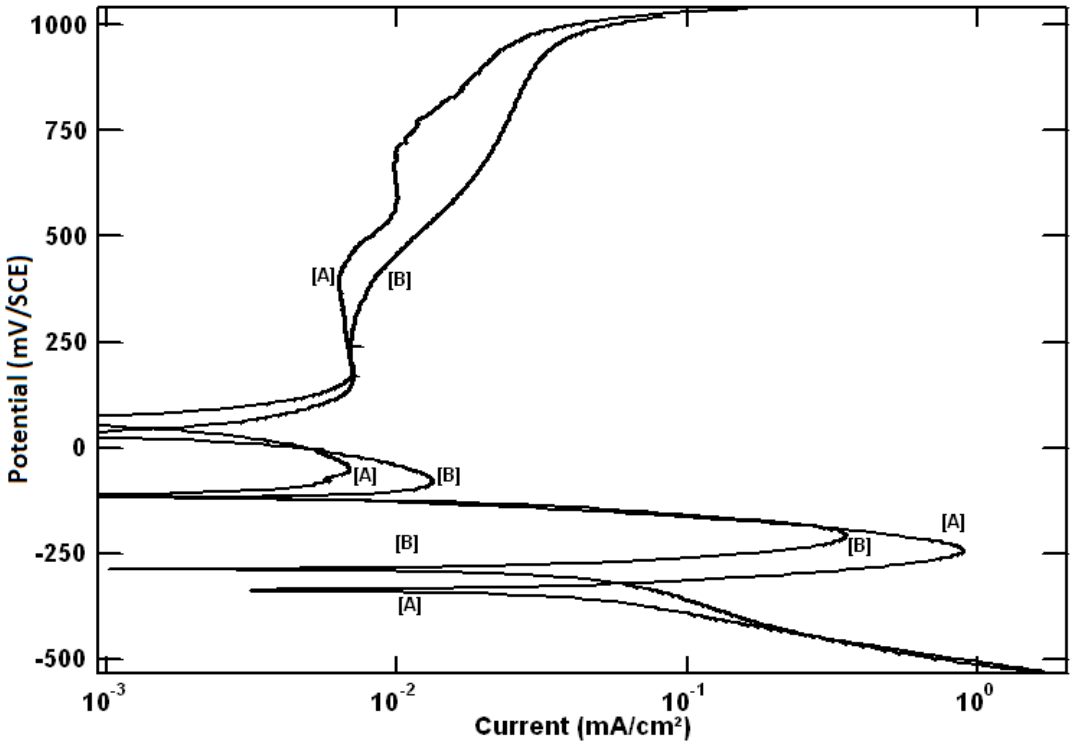

Figure 4. Potentiodynamic polarization curves of 304 SS in [A] 0.5M H_2SO_4 + 0.1M NaCl, [B] 0.5M H_2SO_4 + 0.1M NaCl +10^{-4}M of $KMnO_4$.

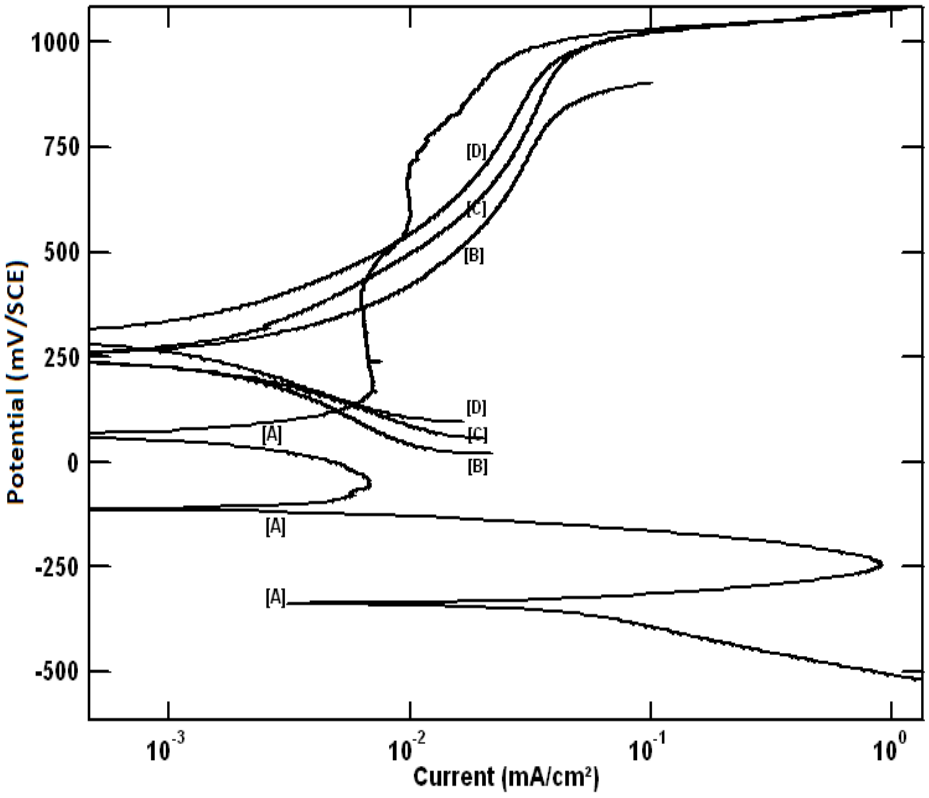

Figure 5. Potentiodynamic polarization curves of 304 SS in 0.5M H_2SO_4 containing 0.1M NaCl in absence and presence of different concentrations of $NaIO_4$; [A] 0, [B] 5 x 10^{-4}, [C]10^{-3}, [D] 10^{-2} M.

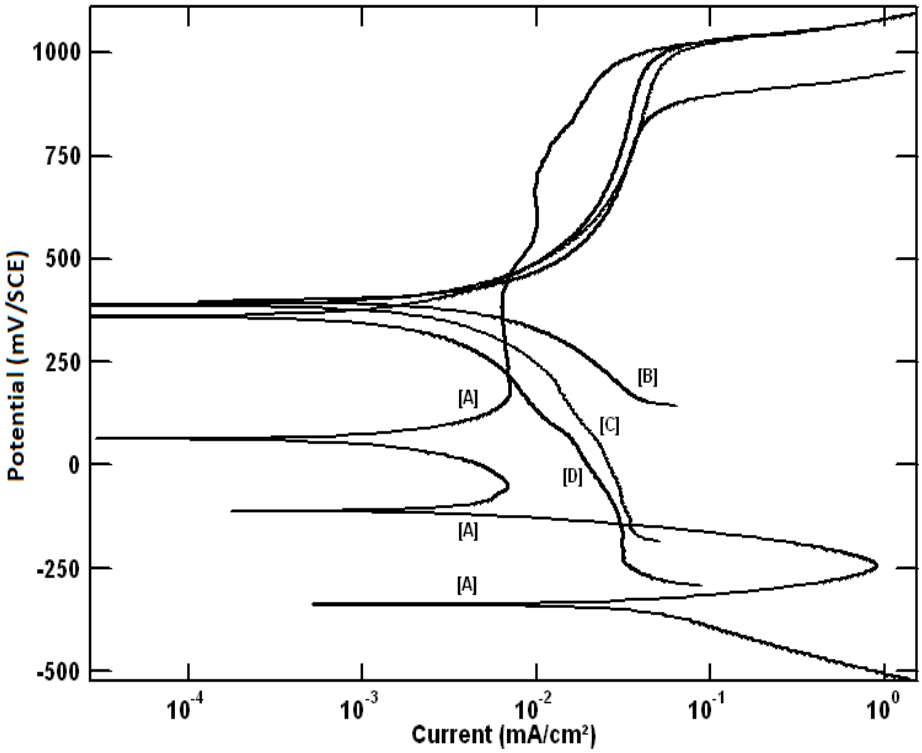

Figure 6. Potentiodynamic polarization curves of 304 SS in 0.5M H_2SO_4 containing 0.1M NaCl in absence and presence of different concentrations of $KMnO_4$; [A] 0, [B] 5 x 10^{-4}, [C] 10^{-3}, [D] 10^{-2} M.

3.2. Electrochemical impedance spectroscopy results

Figure 7 shows the Nyquist plot of 304 SS in 0.5M H_2SO_4 containing 0.1M NaCl in the absence and presence of different concentrations of $Na_2SiO_3.5H_2O$, it is clear that this plot is depressed semicircle of capacitive type. The size of this semicircle increases with increasing silicate ion concentration indicating that the dissolution process of metal occurs under activation control in the absence or presence of silicate ion. Similar Nyquist plot was obtained for SS 304 in sulphuric acid media containing chloride ions [33]

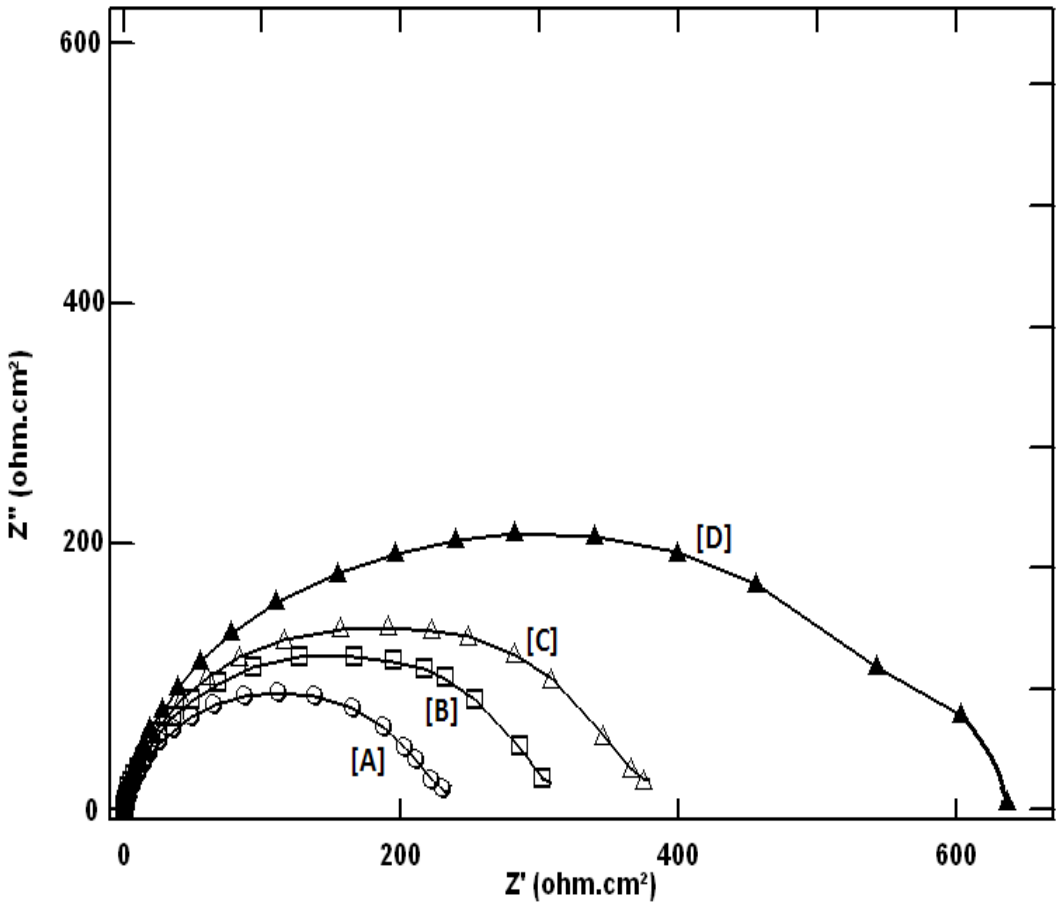

Figure 7. Nyquist plot of 304 SS in 0.5M H_2SO_4 containing 0.1M NaCl in absence and presence of different concentrations of $Na_2SiO_3.5H_2O$; [A] 0, [B] 10^{-4}, [C] 10^{-3}, [D] $3x10^{-3}$ M.

Corrosion rate will be determined by analysis of different Nyquist plots by fitting the experimental data to the following equivalent circuit model, Figure 8, that includes the solution resistance R_s and the double layer capacitance (C_{dl}) which is placed in parallel to charge transfer resistance element, R_{ct} which is inversely proportional to the corrosion rate. Similar equivalent circuit has been used to describe the behavior of SS 304 in the passive state during pit initiation [34]

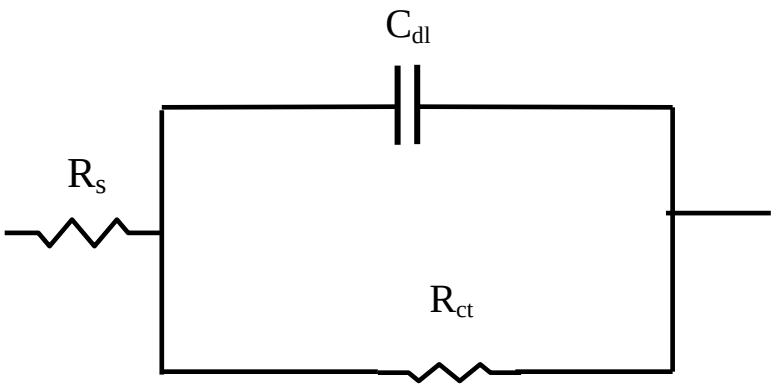

Figure 8. A simple Randles-type equivalent circuit.

Figures 9,10 show the Nyquist plots of 304 SS in 0.5M H_2SO_4 containing 0.1M NaCl in the absence and presence of different concentrations of $NaIO_4$ or $KMnO_4$ respectively. In the absence or presence of low concentration of $NaIO_4$ or $KMnO_4$, it is clear that the impedance response is depressed semicircle of capacitive type indicating that the dissolution of metal is activation-controlled process.

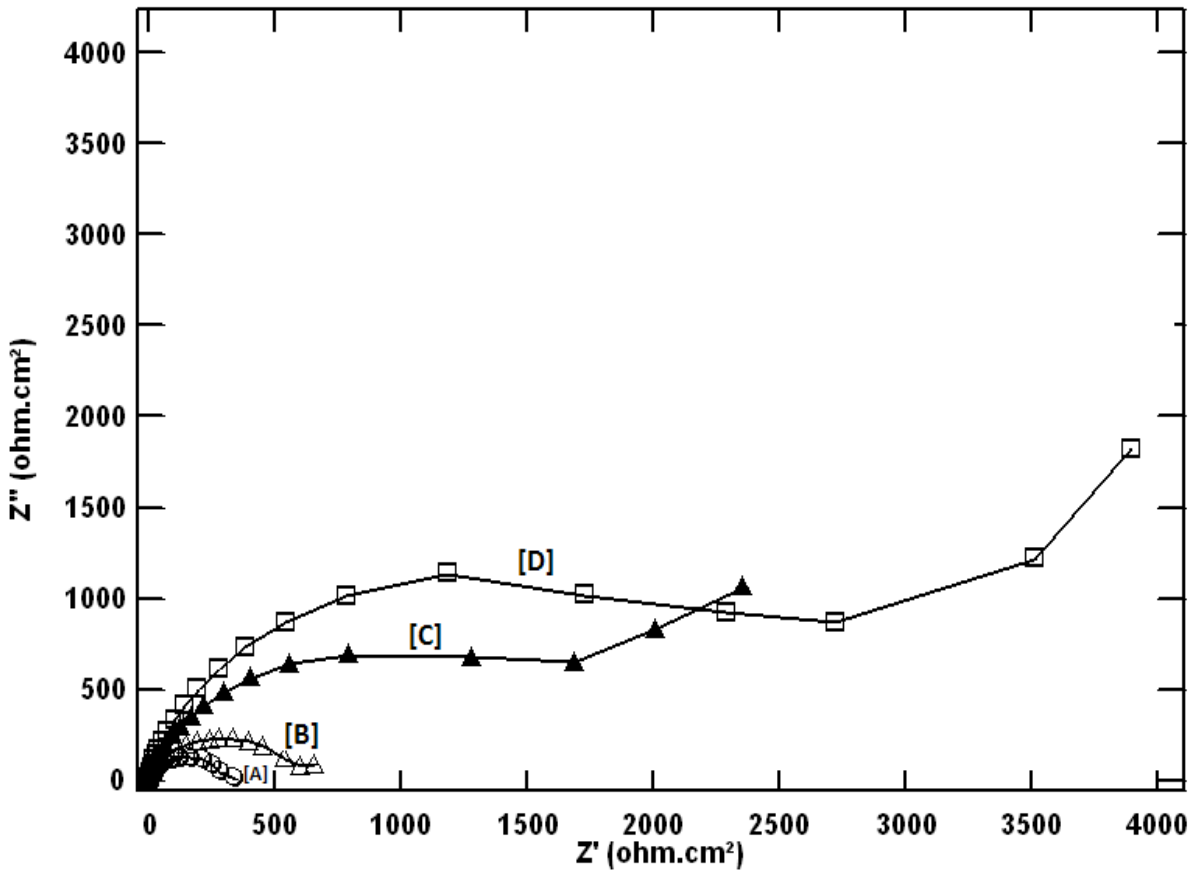

Figure 9. Nyquist plot of 304 SS in 0.5M H_2SO_4 containing 0.1M NaCl in absence and presence of different concentrations of $NaIO_4$; [A] 0, [B] 10^{-4}, [C] $3x10^{-3}$, [D] $4x10^{-3}$ M.

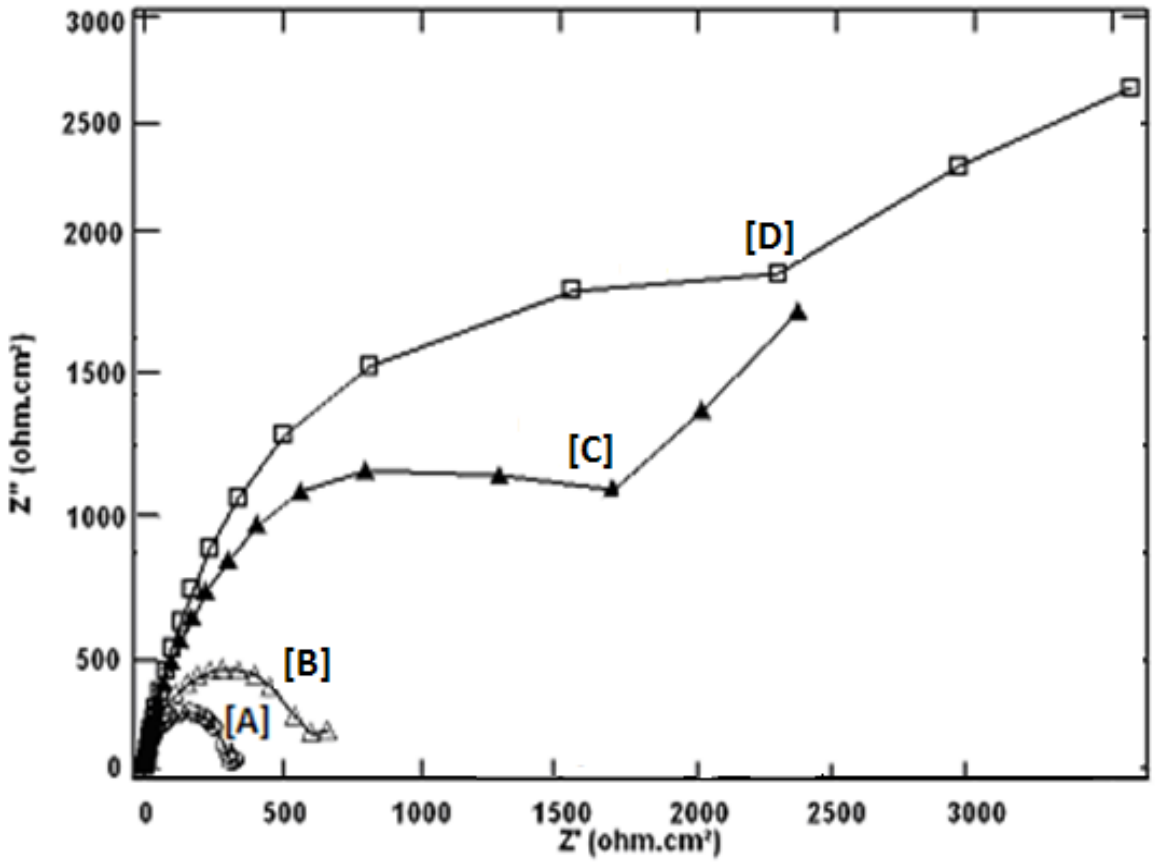

Figure 10. Nyquist plot of 304 SS in 0.5M H_2SO_4 containing 0.1M NaCl in absence and presence of different concentrations of $KMnO_4$; [A] 0, [B] 10^{-4}, [C] $3x10^{-3}$, [D] $4x10^{-3}$ M.

At low concentrations of $NaIO_4$ or $KMnO_4$, analysis of the impedance spectra was executed by fitting the experimental data to the same equivalent circuit model used for silicate, Figure 8. The computer fit results are presented in Table 1. In the presence of high concentration of $NaIO_4$ or $KMnO_4$, the impedance response represents a process that takes place under diffusion control due to the occurrence of the so-called Warburg impedance.

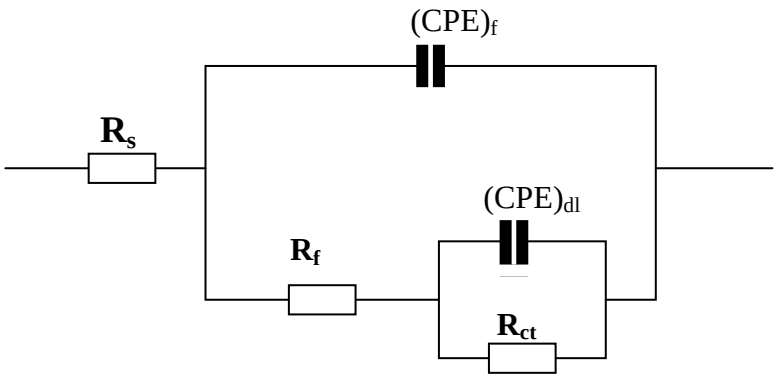

Figure 11: Equivalent circuit used to fit the data at high concentrations of $NaIO_4$ or $KMnO_4$.

The Warburg impedance [35] is observed only at low frequencies and usually describes a mass transfer process involving diffusion of ions. It is known that the diffusion-controlled process distorts the low frequency end of the semicircle. At high concentrations of $NaIO_4$ or $KMnO_4$, analysis of different Nyquist plots was done by fitting the experimental data to the equivalent circuit model, Figure 11.

The equivalent circuit includes the solution resistance (Rs) and the oxide film constant phase element $(CPE)_f$ shorted by a resistive element (R_f) representing the formation of an ionically conductive path across the complex between the electrolyte and the substrate. When an electrolyte penetrates, a double layer is formed at the disbonded region of the complex/metal interface represented by double layer constant phase element $(CPE)_{dl}$ in parallel with the charge-transfer resistance (R_{ct}). Warburg element in the equivalent circuit corresponds to a value of n equals 0.5, impedance response of straight line with a phase angle of 45^o.

Computer fit results to the equivalent circuit, Figure 11 are depicted in Table 1. The electrochemical impedance parameters of 304 SS in 0.5M H_2SO_4 containing 0.1M NaCl in the absence and presence of different concentrations of $Na_2SiO_3.5H_2O$, $NaIO_4$ or $KMnO_4$ are shown in Table 1. The % inh was calculated from impedance measurements using the relation :

$$\% \text{ inh} = [(R_{ct} - R_{cto}) / R_{ct}] \times 100 \quad (1)$$

Where R_{cto} and R_{ct} are the charge transfer resistances in the absence and presence of a given concentration of different anions.

The percent inhibition (%inh) of different concentrations of the anions are also shown in Table 1.

Table 1. Values of R_s, R_{ct}, C_{dl}, and the % inhibition (% inh) of different concentrations of the anions.

Anion	**Silicate**			**Periodate**			**Permanganate**		
Conc (mol/dm^3)	**C_{dl} (µF)**	**R_{ct} ($Ohm.cm^2$)**	**% inh**	**C_{dl} (µF)**	**R_{ct} ($Ohm.cm^2$)**	**% inh**	**C_{dl} (µF)**	**R_{ct} ($Ohm.cm^2$)**	**% inh**
0.00	240	*224*	-	240	224	-	240	224	-
$1x10^{-5}$	215	278	19.4	167	372	39.7	205	415	46.0
$5x10^{-5}$	175	285	21.4	148	410	45.3	189	435	48.5
$1x10^{-4}$	181	292	23.3	129	420	46.7	172	460	51.3
$5x10^{-4}$	142	297	24.6	107	435	48.5	179	480	53.3
$1x10^{-3}$	109	340	34.1	90	575	61.0	101	630	64.4
$2x10^{-3}$	92	435	48.5	68	900	75.1	81	970	76.9
$3x10^{-3}$	86	605	62.9	58	1600	86.0	70	1900	88.2
$4x10^{-3}$	75	705	68.2	38	2200	89.8	59	2900	92.3

The data indicate that the increase of concentration of inorganic anions leads to increasing the charge transfer resistance that is associated with a decrease in C_{dl}. It was previously reported [36] that the adsorption process on the metal surface is accompanied with a decrease in double layer capacitance, this decrease is due to the adsorption of the anion over the metal surface.

The values of inhibition efficiencies follow the following trend:

Permanganate > Periodate > Silicate

This is the same order of oxidizing power of the three anions, this means that permanganate ion has the strongest oxidizing power, consequently, it has the strongest ability to be reduced and hence prevent sulphate reduction reaction.

3.3. Application of adsorption isotherms

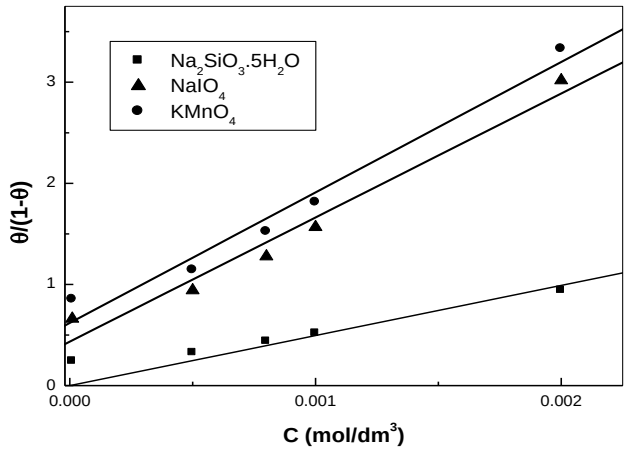

Figure 12. Linear fitting of the data of different anions to Langmuir isotherm.

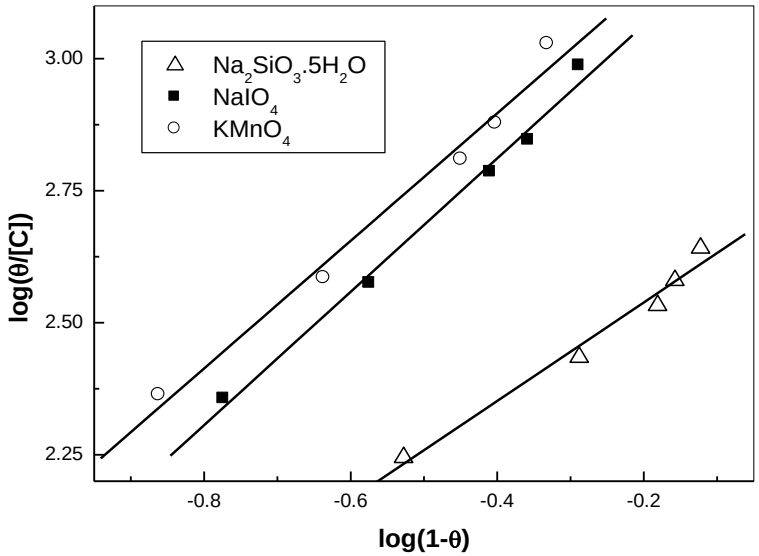

Figure 13. Linear fitting of the data of different anions to Flory- Huggins isotherm.

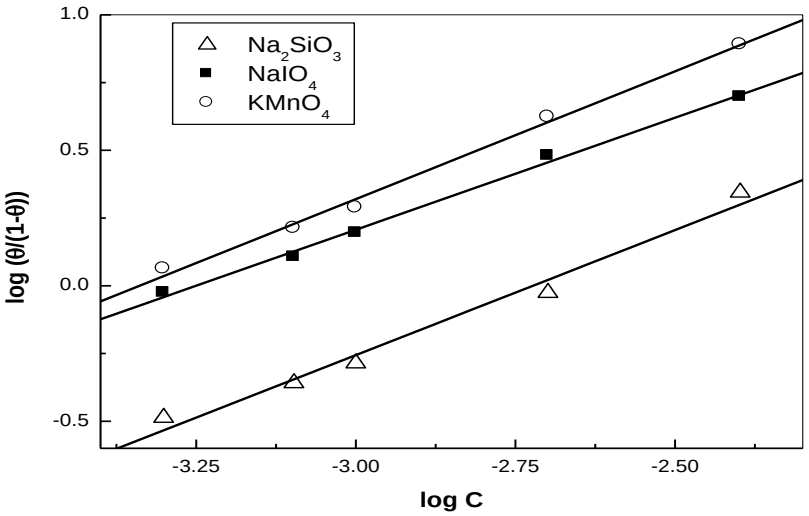

Figure 14. Linear fitting of the data of different anions to Kinetic-Thermodynamic model.

The degree of surface coverage (θ) of the metal surface by an adsorbed anion was calculated using the equation:

$$\theta = (R_{ct} - R_{cto})/R_{ct} \quad (2)$$

Langmuir, Flory Huggins isotherms and Kinetic-Thermodynamic model were used to fit the corrosion data of silicate, periodate and permanganate ions.

The Langmuir isotherm is given by [37]

$$[\theta /(1- \theta)] = K [C] \quad (3)$$

where K is the binding constant, a measure of strength of interaction between the anion and the metal surface and C is the concentration of the anion.

Flory-Huggins isotherm is given by [38]

$$\theta / [x(1- \theta)^x] = K [C] \quad (4)$$

where x is the size parameter, related to the number of adsorbed water molecules substituted by a given inhibitor molecule.

and the kinetic - Thermodynamic model is given by [39]

$$\text{Log } [\theta /(1- \theta)] = \text{Log } K' + y \text{ Log } C \quad (5)$$

where y is the number of inhibitor molecules occupying one active site. The binding constant K is given by:

$$K = K'^{(1/y)} \quad (6)$$

Figures 12-14 show the application of the above mentioned models to the results of adsorption of silicate, periodate and permanganate ions on the stainless steel surface.

The parameters obtained from the Figures are depicted in Table 2.

Applicability of Langmuir isotherm to fit the data of silicate confirms that its adsorption behavior is ideal while inapplicability to fit the data of periodate or permanganate indicates a non-ideal behavior in the adsorption processes [40,41] of the complex of periodate and permanganate ions on the steel surface. Applicability of Flory-Huggins isotherm to the data of the three anions is demonstrated

in Figure 13. The values of the size parameter, x indicated that the adsorbed species of silicate displaces only one water molecule while the adsorbed species of both periodate or permanganate has a large size since they could displace several water molecules from the steel surface [42]. Kinetic-Thermodynamic model is found to fit the data of the three anions.

Table 2. Linear fitting parameters of different anions according to the used models

Anion	Langmuir	Flory Huggins Model		Kinetic-Thermodynamic Model	
	K	X	K	1/y	K
Silicate	515	0.97	541	1.02	524
Periodate	-	1.42	1865	1.39	1805
Permanganate	-	1.48	2180	1.47	2169

The number of active sites occupied by a single inhibitor molecule,1/y was in a good agreement to the size parameter x calculated for the three anions. The values of binding constant, K for silicate obtained from Langmuir and Flory-Huggins isotherms respectively, were equal to that obtained from Kinetic-Thermodynamic model. There is also a good agreement between the binding constant values for periodate and permanganate obtained from Flory-Huggins isotherm and those obtained from Kinetic-Thermodynamic model. The efficiency of a given inhibitor depends on the magnitude of its binding constant so better and stronger interaction is represented by large K values, whereas small values of K indicate weaker metal-inhibitor interaction [43]. The order of decrease of K values obtained from Flory-Huggins isotherm or Kinetic-Thermodynamic models is the same order of decrease of the inhibition efficiency of different anions which is:

Permanganate > Periodate > Silicate

This trend obtained from the application of adsorption isotherms is in a good agreement with that obtained from impedance measurements (Table 1), therefore, the inhibitive effect of anions could be explained by considering the adsorption of the complex formed between the metal and anion on the surface of the native metal acting as a film-forming species decreasing the active area available for acid attack.

4. CONCLUSIONS

- Silicate ion has a moderate effect at all concentrations on the pitting behavior of Stainless steel 304 in 0.5M H_2SO_4 containing 0.1M NaCl.
- Permanganate and periodate ions affect the pitting behavior of Stainless steel 304 in 0.5M H_2SO_4 containing 0.1M NaCl at high concentrations to greater extent than silicate.

ACKNOWLEDGEMENTS
The author wishes to thank Prof. Dr. Beshir Ahmed Abd El-Nabey and Prof. Dr. Ashraf Moustafa, Department of chemistry, Faculty of Science, Alexandria University, Alexandria, Egypt for continuous support and providing advanced instruments and thanks Prof. Dr. Beshir Ahmed Abd El-Nabey for revising the manuscript.

References

1. H.S. Khatak, R. Baldev, Corrosion of Austenitic Stainless Steels: Mechanism, Mitigation and Monitoring. ASM International. Narosa Publishing House: (2002).
2. M. Oberndorfer, M. Kaestenbauer, K. Thayer, Application Limits of Stainless Steels in the Petroleum Industry. SPE 56805, SPE Annual Technical Conference and Exhibition, (October 1999).
3. B.F. Brown, NBS Monograph 156: Stress Corrosion Cracking Control Measures . U.S. Department of Commerce. National Bureau of Standards (1977).
4. A.H. Balk, J.W. Boon and C.F. Etienne, Stress Corrosion Cracking in Austenitic Stainless Steel Fixings for Facade Panels, Br. Corros. J. (Quarterly), 1 (1974) 59.
5. J.E. Truman, *Corros. Sci.*, 17, (1977) 737.
6. C. Tyzack, *Br. Corr. Corros. J.* 7 (1972) 268.
7. A.J. Szyprowski, *Br. Corros. J*. 37 (2002) 141.
8. J.H. Wang, C.C. Su and Z. Szklarska-Smialowska, *Corrosion* 44 (1988) 732.
9. E.A. Abd El Meguid, V.K. Gouda and N.A. Mahmoud, *Mater. Trans. JIM* 35 (1994) 703.
10. V.K. Gouda, E.A. Abd El Meguid, Pitting behaviour of UNS NO 8904 stainless steel in salt solutions, 12th Internaional Corrosion Congress, Texas, USA, 1993, p. 2011–2021.
11. Guocheng LÜ, Haidong CHENG, Chunchun XU, Zonghu HE, *Chinese Journal of Chemical Engineering* 16 (2008) 314.
12. Samir Milad Elsariti, Haftirman, *Procedia Engineering* 53 (2013) 650.
13. T Ujiro, S Satoh, R.W Staehle and W.H Smyrl, *Corros. Sci.*, 43 (2001) 2185.
14. J. Izquierdo, L. Martín-Ruíz, B.M. Fernández-Pérez, R. Rodríguez-Raposo, J.J. Santana and R.M. Souto, *J. Electroanal. Chem*. 728 (2014) 148.
15. F. Zanotto, V. Grassi, A. Balbo, C. Monticelli and F. Zucchi, *Corros. Sci*. 80 (2014) 205.
16. N. Ebrahimi, M.H. Moayed, A. Davoodi, *Corros. Sci.* 53 (2011) 1278.
17. A.M. Al-Mayouf, A.K. Al-Ameery and A.A. Al-Suhybani, *Corrosion* 57 (2001) 614.
18. [A. Galal, N.F. Atta and M.H.S. Al-Hassan, *Mater. Chem. Phys*. 89 (2005) 38.
19. M. Finšgar, S. Fassbender, S. Hirth, and I. Milošev, *Mater. Chem. Phy*. 116 (2009) 198.
20. Yu.Zuo, Haitao wang, Jingmao Zhao and Jinping Xiong, *Corros. Sci*. 44 (2002) 13.
21. N. Ebrahimi, M.H. Moayed and A. Davoodi, *Corros. Sci*. 53 (2011) 1278.
22. F. Eghbali, M.H. Moayed, A. Davoodi and N. Ebrahimi, Corros. Sci. 53 (2011) 513.
23. M.H. Moayed, R.C. Newman, *Corros. Sci*. 48 (2006) 3513.
24. M. Naghizadeh, D. Nakhaie, M. Zakeri and M.H. Moayed, *Corros. Sci.*, *94* (*2015*) *420-427.*
25. M. Zakeri, D. Nakhaie, M. Naghizadeh and M.H. Moayed, *Corros. Sci.*, *93* (*2015*) *234.*
26. Li-Bin Niu, Kensuke Nakada, *Corros. Sci.*, *96* (*2015*) *171*.
27. Pierre, R. Roberge, Handbook of corrosion engineering, Mcgraw-Hill, New York, 2000.
28. D.G. Kolman, D.K. Ford, D.P. Butt and T.O. Nelson, *Corros. Sci*. 39 (1997) 2067.
29. R.T. Loto, J. Environ. Sci. 4(4) (2013) 448-459.
30. G.O Ilevbare' , G.T Burstein, Corros. Sci. 45(7) (2003) 1545–1569.
31. Y. Ait Albrimi, A. Ait Addi, J. Douch, R.M. Souto, M. Hamdani, Corros. Sci.,90 (2015) 522-528.
32. S.A.M. Refaey , F. Taha, A.M Abd El-Malak, Appl. Surf. Sci. 236 (2004) 175–185.
33. P. Q. Zhang, J.X. Wu, W.Q. Zhang , X.Y. Lu and K. Wang, Corros. Sci. 34(8) (1993) 1343-1354.

34. S. Krakowiak, , K. Darowicki, P. Slepski, *Electrochim. Acta*, 50 (13) (2005) 2699–2704.
35. K. Hladky, L.M. Callow and J.L. Dawson, *Br. Corros. J*, 15 (1980) 20.
36. K. Aramaki, M. Hagiwara, and H. Nishihara, *Corros. Sci.* 27 (1987) 487.
37. I. Langmuir, *J. Am. Chem. Soc*. 38 (1916) 2221.
38. P.J. Florry, *J. Chem. Phys*. 10 (1942) 51.
39. A.A. El-Awady, B.A. Abd-El-Nabey and S.G. Aziz, *J. Electrochem. Soc.* 139 (1992) 2149.
40. A.M. Abdel-Gaber, B.A. Abd-El-Nabey, I.M. Sidahmed, A.M. El-Zayady and M. Saadawy, *Corrosion* 62 (2006) 293.
41. A.M. Abdel-Gaber, B.A. Abd-El-Nabey, I.M. Sidahmed, A.M. El-Zayady, M. Saadawy, *Corros. Sci.* 48 (2006) 2765.
42. B.A. Abd-El-Nabey, E-Kamis, M. Sh. Ramadan, and A. El-Gindy, *Corrosion* 52 (1996) 671.
43. N. Khalil, F. Mahgoub, B.A. Abd-El-Nabey, A. Abdel-Aziz, *Corros. Eng. Sci. Technol*., 38 (2003) 205.